Chemical Engineering Journal 160 (2010) 277–283

Contents lists available at ScienceDirect

Chemical Engineering Journal

journal homepage: www.elsevier.com/locate/cej

Self-oscillations in an airlift reactor

Nian Zhang, Tiefeng Wang*, Zhonghuo Deng, Jinfu Wang

Beijing Key Laboratory of Green Reaction Engineering and Technology, Department of Chemical Engineering, Tsinghua University, Beijing, 100084, PR China

ARTICLE INFO

Article history:
Received 18 August 2009
Received in revised form 2 March 2010
Accepted 2 March 2010

Keywords:
Airlift reactor
Self-oscillation
Gas holdup
Liquid circulation velocity

ABSTRACT

Oscillations in the gas holdup and liquid circulation velocity were found at low liquid levels in an airlift reactor with a designed gas–liquid separator. The hydrodynamic behavior and the frequency and amplitude of the oscillations were investigated. The gas holdup and liquid circulation velocity oscillated at the same frequency. The frequency increased from 0.07 to 0.18 Hz with an increase in the superficial gas velocity or liquid level. The gas holdup oscillation occurred mainly in the downcomer. The oscillation amplitude of the average gas holdup in the downcomer was 0.02 at superficial gas velocities of 0.03–0.06 m/s, and was close to zero at other superficial gas velocities. Using the superficial gas velocity and unaerated liquid level, the flow was classified into three regimes: non-circulating regime, self-oscillation regime and completely circulating regime. The self-oscillation regime, determined from the oscillation amplitude, became wider as the liquid level decreased.

1. Introduction

Airlift reactors are now widely used in chemical and environmental processes. They are very promising reactors because of their simple construction, lower shear fields, lower power input, and easier scale-up in comparison with continuous stirred tank reactors [1,2]. Most airlift reactors are operated under steady-state optimal conditions. However, unsteady-state operation has been shown to give a better performance in some processes [3,4]. Periodic operation is a typical unsteady-state operation, and has been widely used in trickle bed [5–8] where a higher time-average conversion of the reactant has been reported [9,10].

An operation with a forced oscillation can be obtained by periodic operating conditions, such as a periodically changing temperature, pressure, flow rate, or concentration. For example, a forced oscillation due to periodically changing the air flow rate was found to significantly improve the oxygen transfer rate in an airlift reactor used for citric fermentation [11]. A forced oscillation can also be obtained by alternately pumping gas into the riser and downcomer, and the gas holdup and gas–liquid mass transfer rate were enhanced [12–14]. The production of yeast cell in an airlift reactor using this operation gave an increased yield of the yeast cells [15].

However, there are few investigations on self-oscillations with a constant gas–liquid flow operation, and these have only been reported for rectangular reactors. A few papers have reported on the oscillation of local gas holdup and liquid velocity in a partly aerated rectangular bubble column with a non-uniform gas distribution [16–19]. An oscillation of the local liquid circulation velocity was observed in a rectangular airlift reactor with two isolated downcomers [20]. However, there has been no report on self-oscillation in the commonly used airlift reactor.

This work reports an experimental study of a self-oscillatory hydrodynamic behavior in an internal airlift reactor with a designed gas–liquid separator. The conditions where self-oscillations occurred were determined. The influences of the superficial gas velocity and liquid level on the oscillation frequency and amplitude were studied. The axial profiles of the oscillating gas holdup were also studied.

2. Experimental

2.1. Apparatus

The experiments were carried out in an internal-loop airlift reactor. The schematic of the experimental apparatus is shown in Fig. 1. The reactor used was made of Plexiglas and comprised four main parts: riser, downcomer, gas distributor and gas–liquid separator. The total height of the reactor was 2.5 m. The riser was surrounded by two coaxial cylinder columns, which were the outer column and the draft tube. The outer column was 0.19 m in inner diameter (i.d.) and 2.02 m in height with a gas–liquid separator on its top. The draft tube was 0.12 m outer diameter, 0.11 m i.d., and 2.0 m in height. Air and tap water were used as the gas and liquid phases, respectively. The air was pumped into the riser through the gas distributor. The difference between the gas holdup in the riser and downcomer was the driving force for the liquid circulation in the reactor.

* Corresponding author.
E-mail addresses: wangtf@tsinghua.edu.cn, wangtf@flotu.org (T. Wang).

1385-8947/$ – see front matter © 2010 Elsevier B.V. All rights reserved.
doi:10.1016/j.cej.2010.03.005

Nomenclature

A	amplitude of the self-oscillation
C	velocity of ultrasound in the medium (m/s)
F	frequency of the self-oscillation (Hz)
f_e	frequency of emitted ultrasound (Hz)
f_r	frequency of received ultrasound (Hz)
f_e	frequency of emitted ultrasound (Hz)
H_L	liquid level (m)
H_{L0}	unaerated liquid level (m)
H	height (m)
P	pressure (Pa)
t	time (s)
U	superficial velocity (m/s)

Greek symbols

ε	phase holdup
ρ	density (kg/m^3)
φ	phase angle

Subscripts

D	downcomer
G	gas phase
L	liquid phase
R	riser
SO	self-oscillation

Two designs of the gas–liquid separator were used. These are shown in Fig. 2. In case A, the downcomer was a single cylinder column. In case B, the downcomer had a gas–liquid separator on its top. The two downcomers had the same diameter and total height. The gas–liquid separator was a cone of diameter 0.12 m at the bottom and 0.27 m at the top. The cone was perforated and connected to three pipes of 0.04 m i.d. as shown in Fig. 2c.

2.2. Liquid level

In an airlift reactor, the liquid level has a significant effect on the flow resistance at the gas–liquid separator, especially when the liquid level is low [21–23]. The liquid level was defined in this work as the height from the top of the draft tube to the free-surface of the liquid. This was noted as H_L for the gas–liquid two-phase flow and H_{L0} for the unaerated liquid, as shown in Fig. 3. When the liquid level was negative, the free-surface of liquid was lower than the top of the draft tube, and there was no liquid circulation.

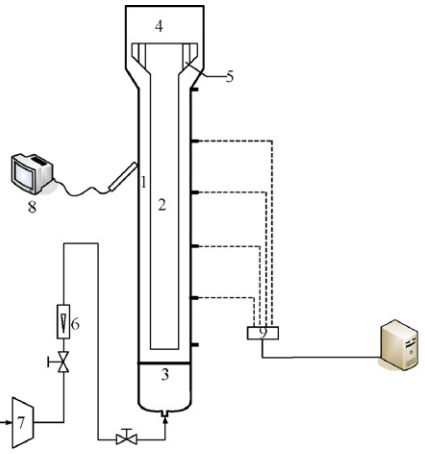

1. Riser; 2. Downcomer; 3. Gas distributor; 4. Enlarged part 5. Gas-liquid separator; 6. Flow meter; 7. Compressor; 8. Ultrasound Doppler velocimetry; 9. Differential pressure transducer

Fig. 1. Schematic of the experimental set-up.

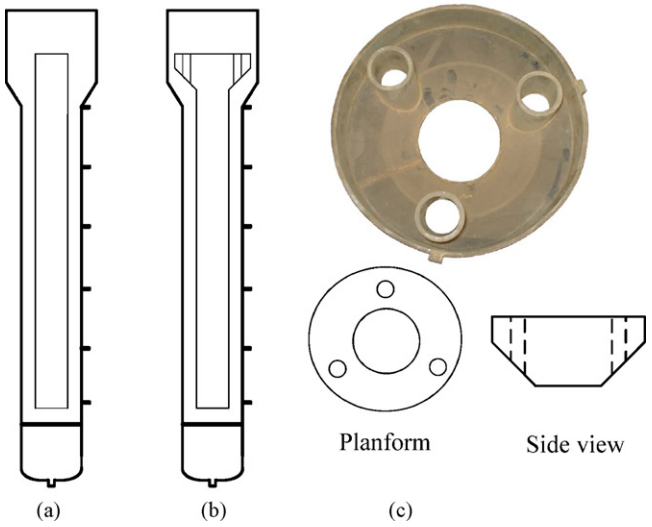

Fig. 2. Schematic of the two types of reactors: Case A: without a gas–liquid separator; Case B: with a gas–liquid separator.

The liquid level where self-oscillation occurred in the airlift reactor was low, and it was difficult to measure it accurately due to the fluctuation of the liquid surface. Moreover, when the liquid level was low, as the liquid in the downcomer was less expanded in the downcomer, the liquid overflowed from the riser and fell down into the downcomer. In such situations, the liquid level was non-uniform in the radial direction, with a higher value near the wall and a lower value in the central region. Due to this, in our experiments, it was the unaerated liquid level that was measured and used as the operating parameter. This is shown in Fig. 3b. The aerated liquid level was higher than the unaerated liquid level, and varied with the superficial gas velocity.

2.3. Measuring methods

2.3.1. Gas holdup

The gas holdup measurements were made both in the riser and downcomer with the differential pressure transducers. The reactor had several tapping ports at positions of 0.1, 0.4, 0.8, 1.2, 1.6 and 2.0 m above the gas distributor in the riser, and 0.05, 0.6, 0.9, 1.2, 1.5 and 1.8 m in the downcomer. Six differential pressure transducers were used to measure the axial profile of the pressure drop. The

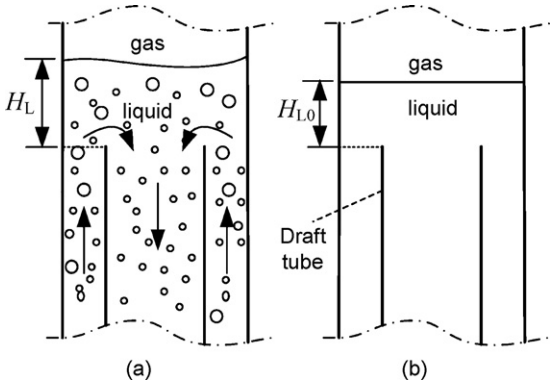

Fig. 3. Schematic of liquid level (H_L in (a)) and unaerated liquid level (H_{L0} in (b)).

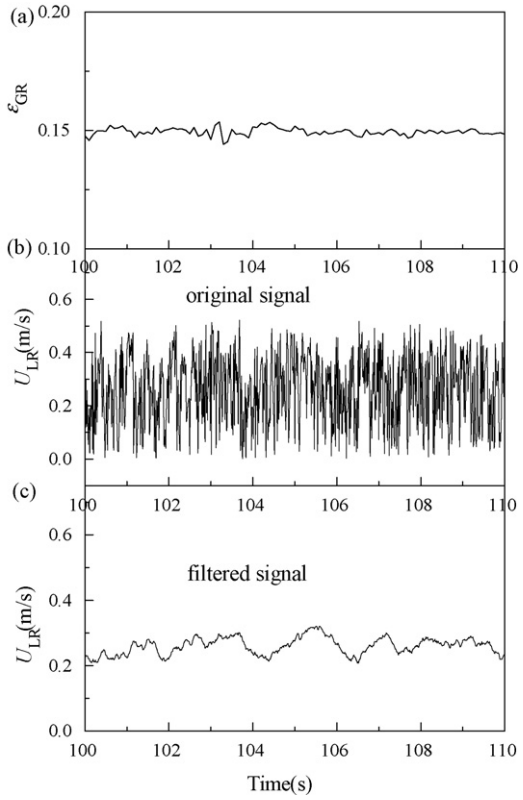

Fig. 4. Measured signal of gas holdup (a), original (b) and filtered (c) signals of liquid circulation velocity.

transducer was connected to the reactor by two pipes filled with water as the pressure transfer medium. The pressure drop due to viscous flow was negligible compared to the static pressure drop, and the pressure drop (ΔP) between two tapping ports with vertical distance h was:

$$\Delta P = \rho_L g h(1 - \varepsilon_G) \tag{1}$$

where ρ_L is the liquid density and ε_G is the gas holdup. From the pressure drop, the gas holdup can be determined using Eq. (2).

$$\varepsilon_G = 1 - \frac{\Delta P}{\rho_L g h} \tag{2}$$

The differential pressure transducer signal was sampled at 10 Hz. The variation of the gas holdup with time was acquired, and shown in Fig. 4a. The global gas holdup in the riser/downcomer was obtained by measuring the pressure drop between the top and bottom of the riser/downcomer through two tapping ports. The local gas holdup was obtained by measuring the pressure drop between two adjacent tapping ports.

2.3.2. Liquid circulation velocity

The liquid circulation velocity (U_L) was measured with an Ultrasound Doppler Velocimetry DOP2000. Typical results are shown in Fig. 4b and c. Ultrasound Doppler velocimetry has been used in the measurement of single phase flow and multiphase flow [24,25] by using the Doppler Effect. When the DOP2000 probe emits an ultrasonic beam, moving particles in the liquid scatter the sound wave. The backscattered sound wave is received by the same sensor probe. The movement of the particle gives the received sound wave a frequency shift (f_{shift}) proportional to the particle velocity (u_p) [24]:

$$f_{shift} = f_e - f_r = \frac{2f_e \left|u_p\right| \cos\theta}{c} \tag{3}$$

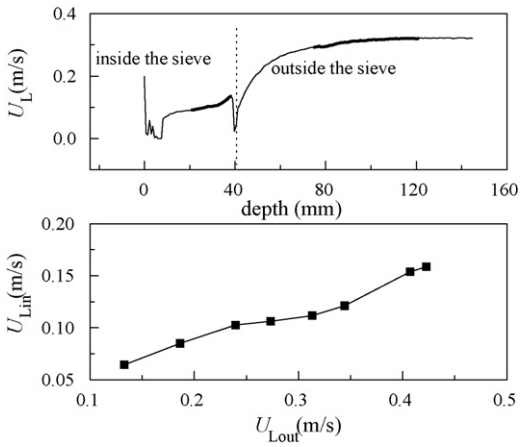

Fig. 5. Effect of the sieve on the flow field near the ultrasound probe.

where f_e, is the emitted sound wave frequency, f_r the received sound wave frequency, θ the angle between the ultrasonic beam and the particle velocity, and c the velocity of sound in the medium. From f_{shift}, the velocity of the particles in the liquid is determined as:

$$\left|u_p\right| = \frac{c f_{shift}}{2 f_e \cos\theta} \tag{4}$$

The DOP2000 is very effective for liquid velocity measurement in single phase flow. However, its use in a gas–liquid two-phase flow is difficult because the bubbles produce a stronger scattering of the sound wave than the tracing particles in the liquid, such that the frequency shift of the received sound wave is mainly due to the bubble velocity. To exclude the effect of gas bubbles, a hollow sieve column was installed at the front of the ultrasound probe. The effect of the sieve on the flow field and the measured liquid velocity was calibrated using a single phase flow. The liquid velocities inside the sieve (U_{Lin}, average distance of 21–37.5 mm from the probe) and outside the sieve (U_{Lout}, average distance of 75–105 mm from the probe) were measured. The relationship between U_{Lin} and U_{Lout} is shown in Fig. 5. During measurements in a gas–liquid two-phase flow, U_{Lin} was measured and U_{Lout} was determined from Fig. 5. The liquid circulation velocity was measured in the riser, with the probe located in the middle of the two walls of the annular riser. The measured time series of the liquid velocity in the gas–liquid flow is shown in Fig. 4b.

2.4. Signal processing

The liquid circulation velocity was measured with a sampling frequency of 100 Hz. Due to flow turbulence and bubble movement, the original signal had a big dispersion. It was filtered by a moving average method. The point in the filtered signal was the average value of 0.5 s original signals. This signal filtration had no effect on the self-oscillation result because the time scale of the self-oscillation was about 10 s, which was much larger than the 0.5 s. The original signal and filtered signal were shown in Fig. 4b and c.

In studying a self-oscillation, the oscillation frequency is an important parameter. The oscillation frequency was obtained from the time series of the gas holdup and liquid circulation velocity using a spectral analysis based on the Short Time Fourier Transform (STFT). A time series of the gas holdup and its power spectrum are shown in Fig. 6. The dominant frequency in the power spectrum is the oscillation frequency, which is 0.160 Hz in Fig. 6b.

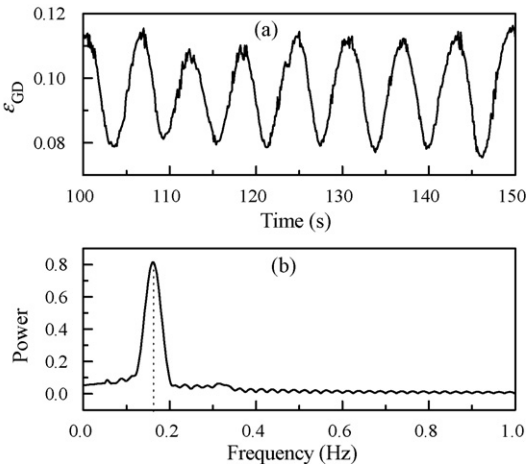

Fig. 6. Power spectrum of the gas holdup time series.

3. Results and discussion

3.1. Characteristics of the self-oscillation

3.1.1. Self-oscillation of the gas holdup

In the airlift reactor with a cone-shaped gas–liquid separator on the top of the downcomer, self-oscillation was observed with the condition of a low liquid level. The time evolution of the global gas holdup in the riser and the downcomer at U_G = 0.03 m/s and an unaerated liquid level H_{L0} = −0.08 m are shown in Fig. 7. The results showed that the global gas holdups in the riser and downcomer had a periodic oscillation. Two stages became dominant alternately: in the first stage, the global gas holdup increased with time and in the second stage, the global gas holdup decreased with time. In a steady-state process, when a disturbance is introduced, its amplitude will decrease and the process will approach a steady-state gradually. However, the oscillation found in this work had a constant amplitude without any forcing oscillation in the input conditions, thus, it was a self-oscillation. The oscillation of the global gas holdup (ε_G) can be correlated as:

$$\varepsilon_G = A\ \sin(2\pi f t + \varphi) + \langle\varepsilon_G\rangle \quad (5)$$

where A, f, φ were the oscillation amplitude, frequency and phase angle, respectively, and $\langle\varepsilon_G\rangle$ is the time-average gas holdup. The gas holdups in the riser (ε_{GR}) and in the downcomer (ε_{GD}) can be correlated as:

$$\varepsilon_{GR} = 0.005\ \sin(0.139 \times 2\pi t + 3.806 + \pi) + 0.117 \quad (6)$$

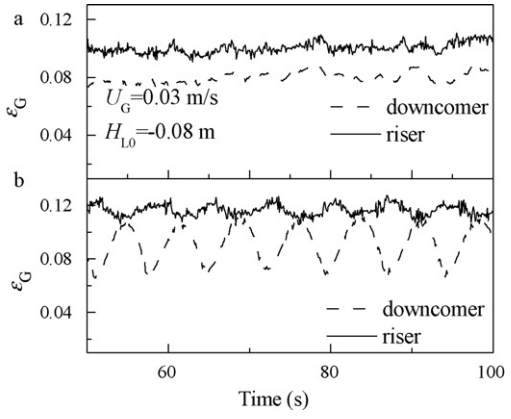

Fig. 7. Gas holdup time series in the different types of reactors. Case A: without a gas–liquid separator; Case B: with a gas–liquid separator.

$$\varepsilon_{GD} = 0.018\ \sin(0.139 \times 2\pi t + 3.844) + 0.091 \quad (7)$$

where the standard deviations of Eqs. (6) and (7) are 0.0035 and 0.0062, respectively.

It was found that the gas–liquid separator determined the existence of self-oscillation phenomenon. When a single cylinder column was used as the draft tube, the gas holdups in the riser and the downcomer fluctuated randomly with time. With a gas–liquid separator installed on the top of the downcomer, self-oscillation of the gas holdup occurred. The reason for the self-oscillation was probably that the bubbles were entrained into the downcomer selectively by the gas–liquid separator. Only bubbles smaller than a certain size can be entrained into the downcomer by the circulating liquid. The decrease in the bubbles in the downcomer caused an increase in the driving force, i.e. the difference between the gas holdups in the riser and downcomer, which led to an increase in the liquid circulation velocity. The driving force and liquid circulation velocity then decreased because more bubbles were entrained into the downcomer. The self-oscillation phenomenon thus appeared. The separation performance and a sufficiently large flow resistance due to the gas–liquid separator were important for producing the self-oscillations in the driving force, gas holdup and liquid circulation velocity.

The gas holdup oscillation resulted in a pressure oscillation. However, this variation in the pressure was different from the pressure fluctuations due to gas bubbles, which has a much higher frequency [26,27].

From Fig. 7, it can be seen that the self-oscillation of the gas holdups in the riser and downcomer had the following characteristics. First, the oscillation was much larger in the downcomer, with its amplitude (A_{SO}) being 3.6 times larger than that in the riser. Second, the oscillations in the riser and downcomer had the same frequency (f_{SO}), but with a phase difference of about π. Although the oscillation of the gas holdup in the downer was significant, the oscillation of the global gas holdup was not significant due to the out-of-phase oscillation in the riser and the larger volume of the riser over that of the downcomer. From the different volumes of the riser and downcomer, the global gas holdup (ε_G) can be calculated from Eqs. (6) and (7) as:

$$\varepsilon_G = 0.0032\ \sin(0.139 \times 2\pi t + 3.84) + 0.108 \quad (8)$$

The liquid level (H) also oscillated in time due to the oscillation of the global gas holdup, with an oscillation amplitude of 0.67 cm.

3.1.2. Axial profile of the gas holdup

Besides temporal oscillation, the gas holdup in the downcomer also showed a complex non-uniform axial profile. Thus, the gas holdup oscillation was a complex spatial-temporal phenomenon. The time evolution of the gas holdups at different axial positions in the downcomer are shown in Fig. 8. The gas holdups at all the axial positions showed oscillation at the same frequency but with different amplitudes and phase angles. They can be correlated with sine functions as:

$$\varepsilon_{GD(1.5-1.8)} = 0.0343\ \sin(0.129 \times 2\pi t + 4.64) + 0.0618 \quad (9)$$

$$\varepsilon_{GD(1.2-1.5)} = 0.0257\ \sin(0.129 \times 2\pi t + 4.12) + 0.0562 \quad (10)$$

$$\varepsilon_{GD(0.9-1.2)} = 0.0234\ \sin(0.129 \times 2\pi t + 2.36) + 0.0401 \quad (11)$$

$$\varepsilon_{GD(0.6-0.9)} = 0.0250\ \sin(0.129 \times 2\pi t + 2.29) + 0.0300 \quad (12)$$

The standard deviations are 0.0121, 0.0075, 0.0077 and 0.0090. Eqs. (9)–(12) fitted the experimental data well. This is shown in Fig. 8. The phase angle of the gas holdup oscillation decreased along the flow direction. The time-average gas holdup in the downcomer was non-uniform in the axial direction. It increased with increasing axial height, as shown in Fig. 9.

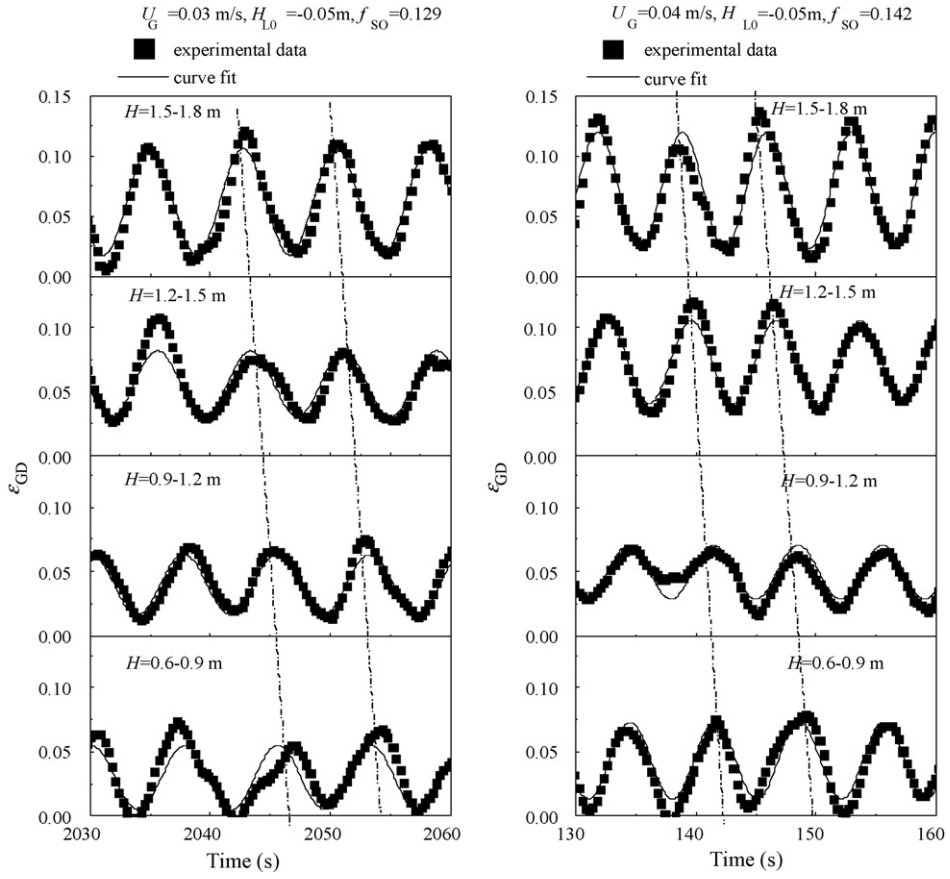

Fig. 8. Gas holdup time series axial distribution in the downcomer (U_G = 0.03 and 0.04 m/s, H_{L0} = −0.05 m).

3.1.3. Self-oscillation of the driving force and liquid circulation velocity

In the airlift reactor, liquid circulation is caused by the difference in the gas holdups in the riser and the downcomer ($\Delta\varepsilon_G = \varepsilon_{GR} - \varepsilon_{GD}$). When the self-oscillation occurred, the driving force $\Delta\varepsilon_G$ also showed an oscillation. The driving force in Fig. 7a can be calculated from Eqs. (6) and (7) as:

$$\Delta\varepsilon_G = 0.023\ \sin(0.139 \times 2\pi t + 0.644) + 0.026 \quad (13)$$

The variation of $\Delta\varepsilon_G$ was from 0.003 to 0.049, which led to a significant variation in the liquid circulation velocity.

The time evolution of the driving force $\Delta\varepsilon_G$ and liquid circulation velocity U_{LR} at U_G = 0.03 m/s and H_{L0} = −0.08 m are shown in Fig. 10. A frequency spectrum analysis was carried out for the oscillations of $\Delta\varepsilon_G$ and U_{LR} using the STFT method. The dominant frequencies for the gas holdup and circulation velocity had the same value of 0.108 Hz.

3.2. Frequency and amplitude of the self-oscillation

3.2.1. Frequency of the self-oscillation

The effects of the superficial gas and unaerated liquid level on the frequency of the self-oscillation (f_{SO}) are shown in Fig. 11. It can be seen that f_{SO} increased with an increase in the superficial

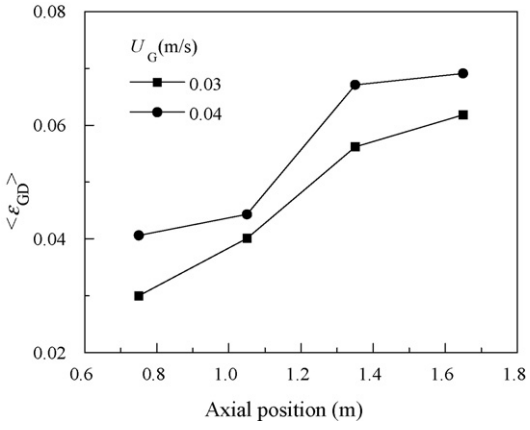

Fig. 9. Axial profile of the time-average gas holdup in the downcomer with a gas–liquid separator.

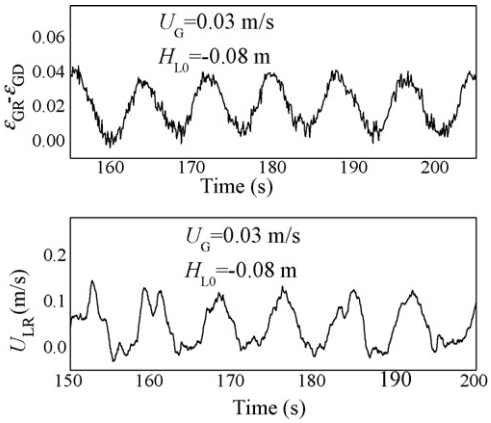

Fig. 10. Oscillation of $\Delta\varepsilon_G$ and U_{LR} (U_G = 0.03 m/s, H_{L0} = −0.08 m).

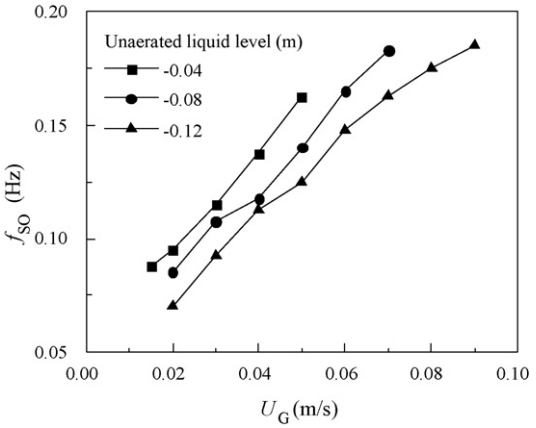

Fig. 11. Effect of the superficial gas velocity and unaerated liquid level on the frequency of self-oscillation of the gas holdup.

gas velocity, and decreased with an increase in the unaerated liquid level. It is worth noting that f_{SO} was approximately proportional to the superficial gas velocity in the self-oscillation regime.

In gas–liquid flow, pressure fluctuations are caused by two different effects [16–19,28]. One is the macro-scale liquid circulation with low frequency oscillations of 10^{-1} to 10^{0} Hz. The other cause is from bubble-scale dynamic behavior that causes high frequency oscillations of 10^{0}–10^{1} Hz. The frequency found in this work was from 0.07 to 0.18 Hz, which was in the range of the liquid circulation.

3.2.2. Amplitude of the self-oscillation

The amplitude of the self-oscillation, A_{SO}, depended on the superficial gas velocity and unaerated liquid level. This is shown in Fig. 12a. It can be seen that A_{SO} of the gas holdup can be divided into three stages with an increase in the superficial gas velocity. At low superficial gas velocities (Stage I), A_{SO} of the gas holdup increased from 0 to around 0.02, and the flow changed from the non-circulating regime to the self-oscillation regime. In Stage II, the flow was in the typical self-circulating regime and A_{SO} showed a constant value between 0.15 and 0.2. In Stage III, A_{SO} decreased to zero with a further increase in the superficial gas velocity, and the flow changed from the self-oscillation regime to the completely circulating regime. The A_{SO} of the liquid circulation velocity had similar characteristics to the A_{SO} of the gas holdup in Stages I and III, as shown in Fig. 12b. However, it decreased in Stage II with an increase in U_G.

Fig. 12 also shows that the unaerated liquid level had a significant influence on A_{SO}. When the unaerated liquid level was zero or higher, the maximum value of A_{SO} became much smaller, and the self-oscillation disappeared gradually. With a decrease in the unaerated liquid level, the transition from the non-circulating regime to the self-oscillation regime was delayed until there was a higher superficial gas velocity, and the range of the self-circulation regime became wider. When the unaerated liquid level was lower than a critical value, A_{SO} of the gas holdup had an approximately non-changing value at different unaerated liquid levels.

The superficial gas velocity and unaerated liquid level are the two important operating parameters that affect the flow regimes. In this work, the lower and upper limits of the self-oscillation regime were determined as the superficial gas velocities at half the maximum amplitude of the oscillation. Fig. 13 shows the flow regimes marked by the superficial gas velocity and unaerated liquid level. At low superficial gas velocity without gas circulating in the downcomer, the flow was in the non-circulating regime (regime I). With an increase in the superficial gas velocity, the flow entered the self-oscillation regime (regime II). With a further increase in the

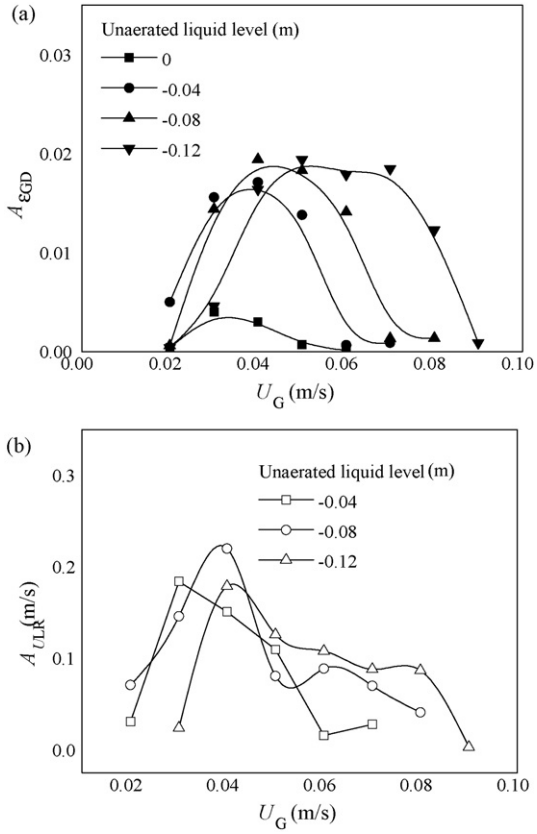

Fig. 12. Effect of the superficial gas velocity and unaerated liquid level on the amplitude of the self-oscillation of the gas holdup in the downcomer (a) and liquid circulation velocity (b).

superficial gas velocity, the flow entered the complete circulating regime (regime III). The flow regime map can be used to identify the flow type in this reactor for specific operation conditions. The non-circulating regime should be avoided for a better performance of the reactor, especially for a gas–liquid–solid system to realize uniform suspension of the solid particles.

3.3. Effect of self-oscillation on the gas holdup

The self-oscillation phenomena had a significant effect on the hydrodynamic behavior of the reactor. The variation of the time-average gas holdup in the downcomer, $\langle \varepsilon_{GD} \rangle$, with U_G is shown in Fig. 14. The unaerated liquid levels were −0.04 m (Fig. 14a) and −0.08 m (Fig. 14b). The gas holdup increased with an increase

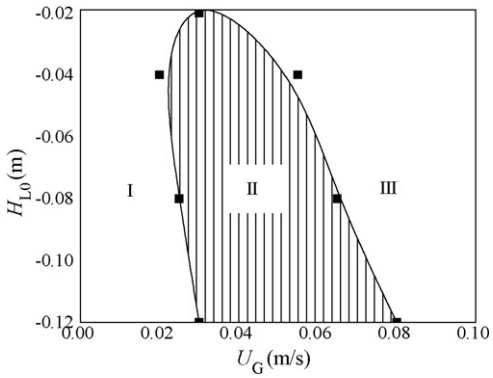

Fig. 13. Flow regime map: (I) non-circulating regime; (II) self-oscillation regime; (III) completely circulating regime.

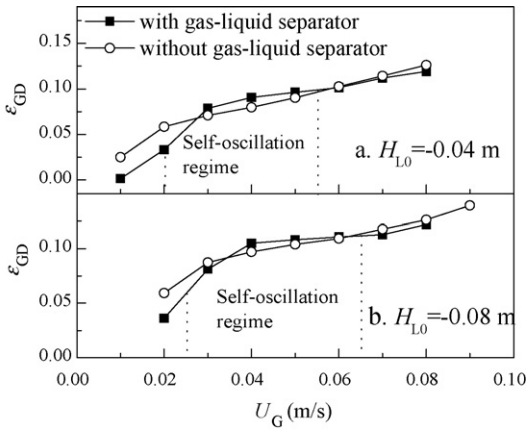

Fig. 14. Effect of the oscillation on the gas holdup.

in the superficial gas velocity. At an unaerated liquid level of −0.04 m, $\langle\varepsilon_{GD}\rangle$ was lower in the reactor with a gas–liquid separation downcomer in the non-circulating regime (U_G: 0.01–0.027 m/s) and completely circulating regime (U_G: 0.058–0.08 m/s), but was higher in the self-circulation regime (U_G: 0.027–0.058 m/s). The situation was similar at H = −0.08 m/s, that is, $\langle\varepsilon_{GD}\rangle$ was higher in the reactor with a gas–liquid separation downcomer in the self-circulation regime (U_G: 0.034–0.063 m/s). This indicates that the self-oscillation enhanced the gas holdup in the downcomer.

4. Conclusions

A self-oscillation phenomenon in an airlift reactor was characterized by the frequency and amplitude of the gas holdup and liquid circulation velocity. The main conclusions are as follows.

(1) A self-induced oscillation existed in an airlift reactor with a designed gas–liquid separator within a specific range of superficial gas velocity at a low unaerated liquid level.
(2) When the self-oscillation occurred, the time evolution of the gas holdup and liquid circulation velocity can be described by a sine function. The oscillation amplitude of the gas holdup in the downcomer was 3.6 times larger than that in the riser. The gas holdup at different axial positions oscillated with the same frequency, but with different amplitudes and phase angles.
(3) The self-oscillations of the gas holdup and liquid circulation velocity had the same frequency that increased from 0.07 to 0.18 Hz with an increase in the superficial gas velocity. The oscillation amplitude of the gas holdup in the self-oscillation regime was about 0.02.
(4) The self-oscillation regime depended on the superficial gas velocity and unaerated liquid level. For an unaerated liquid level of −0.04 m, the self-oscillation regime existed in the superficial gas velocity 0.02–0.06 m/s. The gas velocity range became wider with a decrease in the unaerated liquid level.
(5) Gas holdup in the downcomer was enhanced in the self-oscillation regime.

Acknowledgements

The authors gratefully acknowledge the Foundation for the Author of National Excellent Doctoral Dissertation of PR China (No. 200757), and National 973 Project of China (No. 2007CB714302). They are grateful to Prof. D.Z. Wang for his helpful discussion.

References

[1] M.L. Liu, T.F. Wang, W. Yu, J.F. Wang, Hydrodynamics of a slurry airlift reactor at high solid concentrations, Chem. Eng. Sci. 62 (2007) 7098–7106.
[2] T.F. Wang, J.F. Wang, Y. Jin, Slurry reactors for gas-to-liquid processes: a review, Ind. Eng. Chem. Res. 46 (2007) 5824–5847.
[3] J.M. Douglas, Periodic reactor operation, Ind. Eng. Chem. Process Des. Dev. 6 (1967) 43–48.
[4] P.L. Silveston, Periodic operation of chemical reactors—a review of the experimental literature, Sadhana-Acad. Polit. Eng. Sci. 10 (1987) 217–246.
[5] M.A. Ayude, O.M. Martinez, M.C. Cassanello, Modulation of liquid holdup along a trickle bed reactor with periodic operation, Chem. Eng. Sci. 62 (2007) 6002–6014.
[6] A.T. Castellari, P.M. Haure, Experimental-study of the periodic operation of a trickle-bed reactor, AlChE J. 41 (1995) 1593–1597.
[7] P.M. Haure, R.R. Hudgins, P.L. Silveston, Periodic operation of a trickle-bed reactor, AlChE J. 35 (1989) 1437–1444.
[8] R. Lange, J. Hanika, D. Stradiotto, R.R. Hudgins, P.L. Silveston, Investigations of periodically operated trickle-bed reactors, Chem. Eng. Sci. 49 (1994) 5615–5621.
[9] R. Lange, R. Gutsche, J. Hanika, Forced periodic operation of a trickle-bed reactor, Chem. Eng. Sci. 54 (1999) 2569–2573.
[10] H. Yamada, S. Goto, Periodic operation of trickle bed reactor for hydrogenolysis in gas–liquid–liquid–solid four phases, J. Chem. Eng. Jpn. 30 (1997) 478–483.
[11] S. Godo, J. Klein, M. Polakovic, V. Bales, Periodical changes of input air flowrate—a possible way of improvement of oxygen transfer and liquid circulation in airlift bioreactors, Chem. Eng. Sci. 54 (1999) 4937–4943.
[12] D.H. Liu, F.X. Ding, C.J. Zhang, N.J. Yuan, A study of mass transfer behavior in the two-cell gas–liquid–solid reactor, J. Chem. Eng. Chin. Univ. (Chin.) 3 (1989) 74–79.
[13] T.Z. Liu, D.H. Liu, F. Ouyang, Mass transfer behaviour in a multi-cell gas–liquid–solid oscillatory reactor, Chin. J. Proc. Eng. 17 (1996) 138–143.
[14] Y.Y. Xu, D.H. Liu, D.M. Xie, Study on the effects of forced oscillating period on mass transfer characteristic in airlift loop reactor, J. Chem. Eng. Chin. Univ. (Chin.) 16 (2002) 13–16.
[15] D.H. Liu, S. Huang, M. Li, Y. Sun, T.Z. Liu, F. Ouyang, G.T. Tsao, Improvement of productivity of yeast cell with a novel airlift loop reactor, Appl. Biochem. Biotechnol. 57–8 (1996) 593–598.
[16] V.V. Buwa, V.V. Ranade, Characterization of dynamics of gas–liquid flows in rectangular bubble columns, AlChE J. 50 (2004) 2394–2407.
[17] S. Becker, H. De Bie, J. Sweeney, Dynamic flow behaviour in bubble columns, Chem. Eng. Sci. 54 (1999) 4929–4935.
[18] V.V. Buwa, V.V. Ranade, Dynamics of gas–liquid flow in a rectangular bubble column: experiments and single/multi-group CFD simulations, Chem. Eng. Sci. 57 (2002) 4715–4736.
[19] D. Pfleger, S. Gomes, N. Gilbert, H.G. Wagner, Hydrodynamic simulations of laboratory scale bubble columns fundamental studies of the Eulerian–Eulerian modelling approach, Chem. Eng. Sci. 54 (1999) 5091–5099.
[20] R.S. Oey, R.F. Mudde, H.E.A. van den Akker, Numerical simulations of an oscillating internal-loop airlift reactor, Can. J. Chem. Eng. 81 (2003) 684–691.
[21] M.L. Liu, T.W. Zhang, T.F. Wang, W. Yu, J.F. Wang, Experimental study and modeling on liquid dispersion in external-loop airlift slurry reactors, Chem. Eng. J. 139 (2008) 523–531.
[22] W. Yu, T.F. Wang, M.L. Liu, Z.W. Wang, Bubble circulation regimes in a multistage internal-loop airlift reactor, Chem. Eng. J. 142 (2008) 301–308.
[23] K.H. Choi, Effect of unaerated liquid height on hydrodynamic characteristics of an external-loop airlift reactor, Chem. Eng. Commun. 189 (2002) 23–39.
[24] T.F. Wang, J.F. Wang, F. Ren, Y. Jin, Application of Doppler ultrasound velocimetry in multiphase flow, Chem. Eng. J. 92 (2003) 111–122.
[25] J. Bouillard, B. Alban, P. Jacques, C. Xuereb, Liquid flow velocity measurements in stirred tanks by ultra-sound Doppler velocimetry, Chem. Eng. Sci. 56 (2001) 747–754.
[26] W.H. Zhang, X.G. Li, Origin of pressure fluctuations in an internal-loop airlift reactor and its application in flow regime detection, Chem. Eng. Sci. 64 (2009) 1009–1018.
[27] C. Vial, E. Camarasa, S. Poncin, G. Wild, N. Midoux, J. Bouillard, Study of hydrodynamic behaviour in bubble columns and external loop airlift reactors through analysis of pressure fluctuations, Chem. Eng. Sci. 55 (2000) 2957–2973.
[28] M.E. Diaz, F.J. Montes, M.A. Galan, Experimental study of the transition between unsteady flow regimes in a partially aerated two-dimensional bubble column, Chem. Eng. Process. 47 (2008) 1867–1876.